Spin relaxation rates in quasi-one-dimensional coupled quantum dots

C. L. Romano,[1,*] P. I. Tamborenea,[1] and S. E. Ulloa[2]
[1]*Department of Physics "J. J. Giambiagi," University of Buenos Aires, Ciudad Universitaria, Pab. I, C1428EHA Buenos Aires, Argentina*
[2]*Department of Physics and Astronomy, and Nanoscale and Quantum Phenomena Institute, Ohio University, Athens, Ohio 45701-2979, USA*
(Received 26 May 2006; revised manuscript received 7 August 2006; published 27 October 2006)

We study theoretically the electron-spin relaxation rate in quasi-one-dimensional coupled semiconductor quantum dots. The cross-sectional confinement or shape of these nanorods can be chosen so that either the Rashba or the Dresselhaus spin-orbit coupling is present. We consider acoustic-phonon-mediated transitions between the ground state and the next two higher-energy eigenstates. These three states are nondegenerate due to the interdot coupling, which causes a symmetric-antisymmetric gap, and a competition with the Zeeman splitting. With Rashba coupling and at fixed Zeeman splitting the two upper states display an anticrossing versus interdot barrier width, which is shown to be associated with a sharp cusp in the spin relaxation rate.

DOI: 10.1103/PhysRevB.74.155433 PACS number(s): 73.21.Hb, 72.25.Rb, 73.21.−b, 71.70.Ej

I. INTRODUCTION

Spin-related phenomena in semiconductors attract much attention as they are the foundation of the emerging fields of spintronics[1] and quantum computing in semiconductor systems.[2] Quantum dots (QDs) are particularly promising since they offer relatively long spin coherence times, a key requirement in quantum information processing. Electron-spin relaxation in QDs has been studied recently theoretically[3–24] and experimentally.[25–29] In this paper, we report calculations of spin relaxation rates in coupled double QDs, a type of structure that offers a useful control parameter, i.e., the interdot separation, or barrier width. In particular, we consider here quasi-one-dimensional (quasi-1D) dot structures produced in nanowhiskers or nanorods studied experimentally.[30–34] We have recently studied the electronic states of such quasi-1D double dots, and analyzed their spin-mixed character, which arises from the spin-orbit (SO) interaction.[35] An interesting and potentially useful characteristic of these QD structures is that they can be designed so that only the Rashba or the Dresselhaus spin-orbit couplings are present in a given structure.[35] Therefore, they lend themselves ideally to the experimental study of the individual spin-orbit couplings, which is a desirable feature in quantum dot systems.[22]

In this paper, we calculate rates of spin-flip transitions induced by phonon scattering between Rashba spin-mixed states, taking into account the different acoustic-phonon modes present in zinc-blende semiconductors. Strictly speaking, as we shall see below, the quantum transitions between the ground state and the next two excited states of the structures can reasonably be termed spin-flip transitions only for certain ranges of values of the interdot barrier width, due to the spin-mixed nature of the first and second excited states. On the other hand, the phonon-mediated transitions between quantum states in the presence of only the Dresselhaus coupling are never spin-flip transitions, due to the fact that in these quasi-1D structures the Dresselhaus coupling is proportional to S_z and therefore does not couple the up and down spin states.

In the case where the Rashba coupling is active we find that the relaxation rate shows a strong dependence on the interdot-barrier width and can, furthermore, be tuned with an external magnetic field. This provides interesting flexibility in the control of electronic spin states and spin-flip rates. As we will see, the double-well structure provides an interesting system where the competition between the symmetric-antisymmetric gap and the Zeeman splitting has important consequences. The appearance of level anticrossings in the spectrum, whenever these two energy scales coincide, produces strongly varying spin transition rates: a cusp in the rate vs barrier width which shifts for different magnetic fields.

Similar cusps have been reported in other dot systems and are due to geometrical effects.[22,36] Apart from the different physical nature of the level anticrossing giving rise to the cusp reported here, one important feature of this effect is that it can be accessed dynamically in a given system by varying the applied magnetic field. It is also interesting that there is such a strong dependence on structure and applied fields for double quantum dots such as these, especially considering that coupled dot systems are ubiquitous in a number of proposals for quantum gates.

The paper is organized as follows. In Sec. II we describe the systems studied and the calculation of the relaxation rates. In Sec. III the main results of the study are given, and in Sec. IV we provide concluding remarks.

II. QUANTUM DOT SYSTEM AND RELAXATION RATES

Let us denote by z the coordinate in the longitudinal direction of the quasi-1D coupled double-quantum-dot structure. $V_z(z)$ is the confining potential that defines the pair of coupled QDs. In Fig. 1 we show $V_z(z)$ for an InSb-based structure along with the four bound single-particle states, located next to their corresponding energy levels. We assume that each dot has a length of 30 nm, and we take the width of the barrier between dots, b, as a variable parameter. The nanorod width (cross section) is roughly ten times smaller than the dots' length. Introducing a weak magnetic field in the z direction that breaks the spin degeneracy (but produces

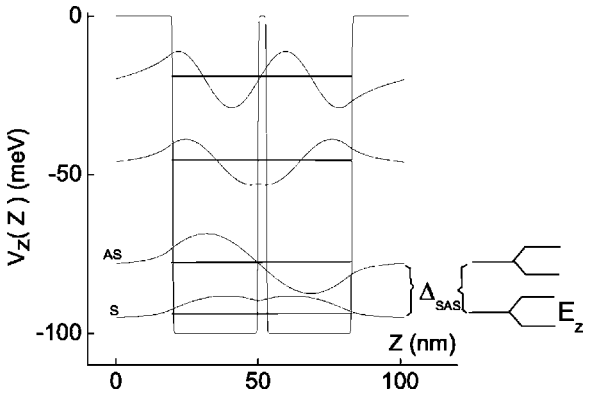

FIG. 1. Potential energy in the longitudinal direction of an InSb-based double-dot structures. The energy levels and eigenfunctions are shown. The energy difference between the lowest symmetric and antisymmetric states is called Δ_{SAS}. The Zeeman energy E_z is also illustrated when a field along z is present.

no significant diamagnetic shift), the Hamiltonian takes the form[35,37,38]

$$H = \frac{\mathbf{P}^2}{2m^*} + V_z(z) + H_{SO} + H_Z, \tag{1}$$

where $\mathbf{P}=(P_x,P_y,P_z)$, $\sigma=(\sigma_x,\sigma_y,\sigma_z)$ is the Pauli matrix vector, and $H_Z=\frac{1}{2}g\mu_B B\sigma_z$ is the Zeeman term.[40] The three-dimensional problem is reduced to an efective one-dimensional problem by taking the average, denoted in what follows by $\langle\cdots\rangle$, over the ground states of the lateral confining potentials.[35,39] One obtains the following effective one-dimensional Hamiltonian:

$$H_{1d} = \frac{p_z^2}{2m^*} + V_z(z) + H_Z + H_{1dD} + H_{1dR}, \tag{2}$$

$$H_{1dD} = \frac{\gamma_D}{\hbar^3}(\langle p_x^2\rangle - \langle p_y^2\rangle)\sigma_z p_z, \tag{3}$$

$$H_{1dR} = \frac{\gamma_R}{\hbar}\left(\left\langle\frac{\partial V_y}{\partial y}\right\rangle\sigma_x - \left\langle\frac{\partial V_x}{\partial x}\right\rangle\sigma_y\right)p_z, \tag{4}$$

where H_{1dD} is the one-dimensional Dresselhaus term, and H_{1dR} is the Rashba-like term enabled by the inversion asymmetry of the laterally confining potentials V_x and V_y. γ_R and γ_D are parameters that depend on the materials.

We diagonalize the Hamiltonian to take full account of the SO effects. We consider two cases for the lateral confining potentials $V_x(x)$ and $V_y(y)$.[35]

(i) $V_x(x)=V_y(y)$ without inversion symmetry, so that the Dresselhaus terms cancel out while the Rashba terms do not.

(ii) $V_x(x)$ and $V_y(y)$ with inversion symmetry but $V_x(x) \neq V_y(y)$, so that only Dresselhaus terms are present. We take $V_x(x)$ and $V_y(y)$ as parabolic potentials with different curvature.

It is important to note that the one-dimensional Dresselhaus coupling Eq. (3) is proportional to σ_z and therefore does not couple the up and down spin states. Thus, the electron-phonon interaction will be unable to induce spin-flip transitions. Therefore, there is no spin relaxation mediated by electron-phonon interaction for nanorod geometries where only Dresselhaus coupling is active. On the other hand, the Rashba coupling Eq. (4) does mix the spin states and causes a spin admixture in the eigenstates of the system. The electron-phonon interaction can cause in this case transitions between states which can be characterized as spin flips. Our calculations will concentrate mostly on situations where only Rashba coupling is present.

We calculate relaxation rates due to acoustic-phonon scattering between the ground state and the next two energy eigenstates in InSb and GaAs QDs via Fermi's golden rule:

$$\Gamma_{i\to f} = \frac{2\pi}{\hbar}\sum_{\mathbf{Q},\alpha}|\langle f|U_{Q,\alpha}|i\rangle|^2 n\delta(\Delta E - \hbar\omega_\alpha), \tag{5}$$

where $\mathbf{Q}=(q_x,q_y,q_z)=(\mathbf{q},q_z)$ is the phonon momentum; α indicates the acoustic-phonon modes, and can take the values ℓ for longitudinal and t=TA1 and TA2 for transverse modes; $\Delta E=E_f-E_i$; and n is the Bose-Einstein phonon distribution with energy $\hbar\omega_\alpha=\hbar c_\alpha Q$, where c_α is the sound velocity of each mode. The kets $|f\rangle$ and $|i\rangle$ represent the final and initial electronic states obtained by exact (numerical) diagonalization of the Hamiltonian. The potential $U_{q,\alpha}$ includes both deformation $\Xi_\ell(\mathbf{Q})$ and piezoelectric $\Lambda_\ell(\mathbf{Q})$ contributions:[41]

$$U_{q,\alpha=\ell,t} = [\Xi_\ell(\mathbf{Q}) + i\Lambda_{\ell,t}(\mathbf{Q})]e^{i\mathbf{Q}\cdot\mathbf{r}}. \tag{6}$$

For zinc-blende semiconductors, the phonon potentials read (in cylindrical coordinates)[24] $\Xi_\ell(\mathbf{Q})=\Xi_0\sqrt{\frac{\hbar}{2DVc_\ell}}\sqrt{Q}$, $\Lambda_\ell(\mathbf{Q})=\frac{6\pi eh_{14}}{\kappa}\sqrt{\frac{\hbar}{2DVc_\ell}}\sin(2\phi)\frac{q^2q_z}{Q^{7/2}}$, $\Lambda_{\mathrm{TA1}}(\mathbf{Q})=\frac{4\pi eh_{14}}{\kappa}\sqrt{\frac{\hbar}{2DVc_{\mathrm{TA}}}}\times\cos(2\phi)\frac{qq_z}{Q^{5/2}}$, and $\Lambda_{\mathrm{TA2}}(\mathbf{Q})=\frac{2\pi eh_{14}}{\kappa}\sqrt{\frac{\hbar}{2DVc_{\mathrm{TA}}}}\sin(2\phi)\frac{q^3}{Q^{7/2}}\left(2\frac{q_z^2}{q^2}-1\right)$, where Ξ_0 and eh_{14} are the bulk constants, κ is the dielectric constant, D is the mass density, and V is the volume.[42]

We assume throughout this work a temperature of 298 K. When studying systems with Rashba coupling, we take a Rashba structural parameter $\left\langle\frac{\partial V_x}{\partial x}\right\rangle$=5 meV/nm. For simplicity we assume in our rate calculations that the lateral confinement is parabolic without a cutoff due to the finite width of the nanowhisker, and we choose the harmonic frequency so that the wave function has an extent of 2 nm (our results are not sensitive to the precise value of the lateral width within the regime studied here). For InSb- and GaAs-based systems, the wells are taken to be 100 and 220 meV deep, respectively. For the systems with Dresselhaus coupling, we assume harmonic oscillator confinements in the x and y directions, with lengths of 2 and 5 nm, respectively. Other material parameter constants are taken from the literature.[42]

III. RESULTS

Figure 2 shows results of varying the central barrier width b between the dots. For case (ii) above, where only Dresselhaus coupling is present, Fig. 2(a) shows the four lowest energy levels for a double-dot structure, as function of the barrier width b. A magnetic field of B=0.8 T is included. As expected, the second and third levels, which do have oppo-

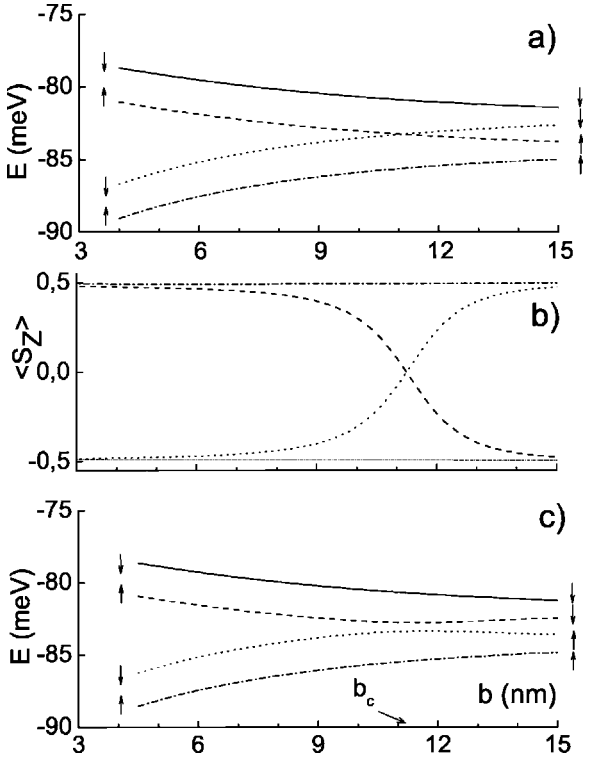

FIG. 2. (a) Energy levels for the four lowest-energy eigenstates as functions of the width of the central barrier, b, for InSb structures with Dresselhaus coupling [case (ii)]. (b) and (c) Mean value of S_z and energy levels, respectively, for structures with Rashba coupling [case (i)]. Level anticrossing occurs only in this case (i). $B=0.8$ T for both types of system. Arrows next to curves indicate spin of state away from the (anti)crossing. Notice Δ_{SAS} gap separates same-spin curves in (a) and (c) and decreases with increasing b.

site spins, do not mix, and only exhibit a true level crossing, as the Dresselhaus coupling in Eq. (3) only shifts spin levels and does not mix states.

In contrast, Figs. 2(b) and 2(c) show the mean values of S_z and the four lowest energy levels, respectively, as functions of the width of the central barrier, b, for double-dot structures with Rashba coupling [case (i) above, and also in the presence of a magnetic field $B=0.8$ T]. Notice in Fig. 2(c) that the second and third levels show an anticrossing at a barrier width where their S_z mean values switch, $b_c(0.8\ \mathrm{T})=11.2$ nm. At low b values, the second state is the spatially symmetric double-dot state with spin down, while the third state is the spatially antisymmetric state with spin up. Increasing barrier width decreases the symmetric-antisymmetric splitting (Δ_{SAS}, shown in Fig. 1), allowing SO coupling to produce strong mixing, which results in the anticrossing and spin switching we see in Figs. 2(b) and 2(c). The same effect could be obtained by varying the barrier height at fixed width. This "crossing value" is, naturally, magnetic field dependent, as the magnetic field controls whenever the Zeeman splitting equals the Δ_{SAS} gap (notice the field is along the z direction or whisker length, and it does not change Δ_{SAS}). We should stress that the differences seen in Figs. 2(a) and 2(c) (crossing vs anticrossing of different spin states) illustrate the striking effect of symmetry of

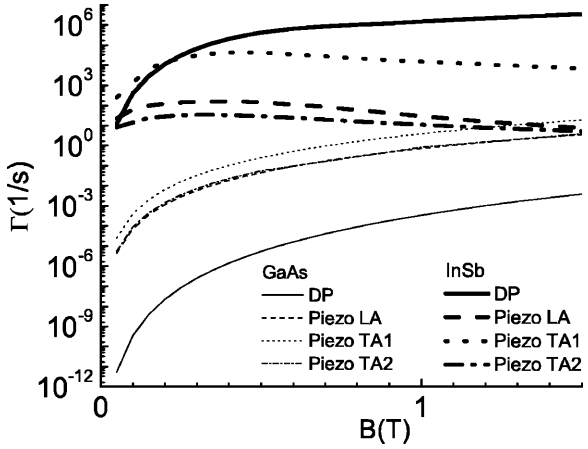

FIG. 3. Spin relaxation rates due to the different acoustic-phonon potentials: deformation (DP), piezoelectric longitudinal (Piezo LA), transverse 1 (Piezo TA1), and transverse 2 (Piezo TA2) potentials, for InSb (thick lines) and GaAs (thin lines) QDs as functions of the applied magnetic field. Here, we consider $b=3$ nm.

the cross-sectional confinement potential of the double-dot system in the nanowhiskers, and the role of spin-orbit coupling. If one could control the x-y confinement potential in the whiskers, one could in principle control the spin mixing and corresponding relaxation rates of the different electronic states. Let us explore this point quantitatively.

Figure 3 shows the contributions to the spin relaxation (SR) rate in InSb and GaAs coupled QDs with only Rashba coupling [case (i)]. The four different acoustic-phonon potentials, deformation, piezoelectric longitudinal (LA), and piezoelectric transverse 1 (TA1) and transverse 2 (TA2) potentials, are studied and compared. The rates shown correspond, more precisely, to the transition between the two lowest-energy states. In InSb QDs, we note that the SR rate is dominated by the deformation potential (for $B>0.3$ T), while in GaAs it is dominated by the piezoelectric TA1 potential (notice, however, that the different contributions are also size dependent[22,24]). Furthermore, in InSb QDs, the contributions from the TA2 and LA potentials can be neglected against those of the other two potentials for magnetic fields beyond

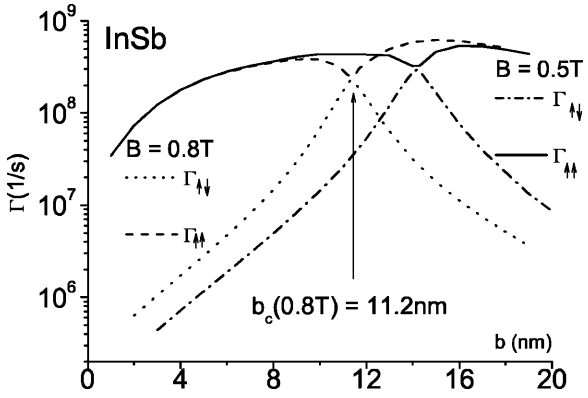

FIG. 4. Relaxation rates as functions of central barrier width in InSb QDs, for two different values of the magnetic field ($B=0.5$ and 0.8 T), and spin-flip ($\Gamma_{\uparrow\downarrow}$), and non-spin-flip ($\Gamma_{\uparrow\uparrow}$) transitions. Rashba coupling is allowed by the confinement symmetry [case (i)].

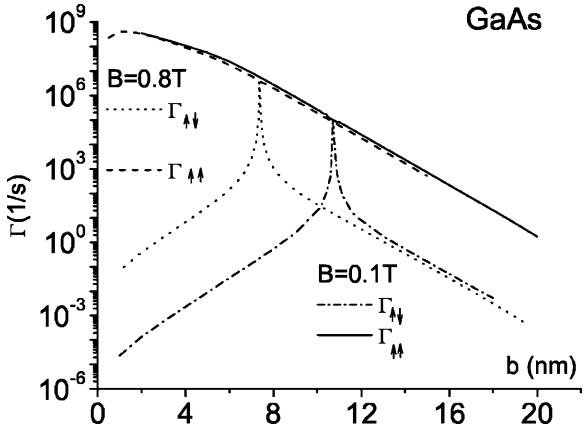

FIG. 5. Same as Fig. 4 but for GaAs at $B=0.1$ and 0.8 T.

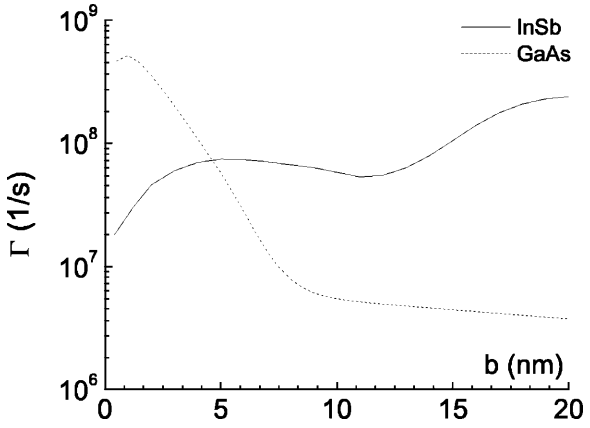

FIG. 6. Phonon-mediated transition rates in structures with Dresselhaus spin-orbit coupling [case (ii)]. Note that the transitions involved do not flip spin, and no cusp appears.

roughly 0.1 T, since they are several orders of magnitude smaller than the latter. The same is true of the deformation potential in GaAs in comparison to the other three potentials. Due to the strong spin-orbit interaction and small band gap of InSb, the SR is in general much larger for that material than for GaAs, as one can observe in Fig. 3.

Figure 4 shows the total transition rate from the first (GS-1) and second (GS-2) excited states to the ground state of InSb QDs, and two values of the magnetic field, $B=0.5$ and 0.8 T, as function of the barrier width b. The up-to-down spin-flip transition corresponds to GS-1 at low b and to GS-2 at high b, and the rate associated with spin flip, $\Gamma_{\uparrow\downarrow}$, is shown as dotted (for $B=0.8$ T) and dash-dotted ($B=0.5$ T) curves. For a given magnetic field, the spin-flip rate shows a cusp at a barrier width that coincides with the crossing width b_c, as introduced in Fig. 2. Accordingly, the cusp position in $\Gamma_{\uparrow\downarrow}$ shifts to lower b values with increasing magnetic field. An analogous situation can be seen in Fig. 5 for GaAs QDs, with $B=0.1$ and 0.8 T. Here the cusp is sharper than for InSb, due to the weaker SO coupling. It must be noted that these are not strictly speaking "spin-flip" transitions, particularly at and around the cusp, since the excited states involved are not spin eigenstates. The rates of the non-spin-flip transitions, $\Gamma_{\uparrow\uparrow}$, on the other hand, show slight dips at the same b_c position, reflecting also the mixed-spin character of the states 1 and 2. The appearance of the cusp on the SR rates clearly arises from the enhanced level mixing when the symmetric-antisymmetric states anticross in the double QD. This effect is similar to that described recently in single quasi-2D dots,[22,24] although in that case the level mixing is associated with anticrossing of different angular momentum states.

For comparison of different spin-orbit mechanisms, Fig. 6 shows the transition rates between the first excited state and the ground state of structures with only Dresselhaus coupling [case (ii)]. As mentioned earlier, these are not spin-flip transitions, but rather regular orbital-type transitions mediated by phonon scattering. It is clear that the sharp cusp present with Rashba coupling does not appear here, since the Dresselhaus spin-orbit does not introduce spin mixing in this geometry, and there is no enhancement of the spin relaxation in turn.

IV. CONCLUSION

To summarize, we have studied the phonon-mediated electronic transitions between Rashba spin-mixed states in GaAs and InSb coupled QDs. The spin relaxation rate shows a cusplike maximum as a function of the separation between the dots. The position of this maximum can be controlled with a small external magnetic field, and can in principle be used to significantly change the electronic SR rates in the system. In contrast, Dresselhaus spin-orbit interaction does not produce spin mixing or spin relaxation.

ACKNOWLEDGMENTS

We thank C. F. Destefani, R. Romo, C. Büsser, and M. Zarea for useful discussions, and support from CMSS at OU, UBACyT, ANPCyT Grant No. 03-11609, and NSF-CONICET through CIAM-NSF Collaboration No. 0336431.

*Electronic address: carlu@df.uba.ar

[1] I. Zutic, J. Fabian, and S. Das Sarma, Rev. Mod. Phys. **76**, 323 (2004).

[2] D. Loss and D. P. DiVincenzo, Phys. Rev. A **57**, 120 (1998).

[3] A. V. Khaetskii and Y. V. Nazarov, Phys. Rev. B **61**, 12639 (2000); **64**, 125316 (2001).

[4] S. I. Erlingsson, Yu. V. Nazarov, and V. I. Fal'ko, Phys. Rev. B **64**, 195306 (2001).

[5] I. A. Merkulov, Al. L. Efros, and M. Rosen, Phys. Rev. B **65**, 205309 (2002).

[6] C. Tahan, M. Friesen, and R. Joynt, Phys. Rev. B **66**, 035314 (2002).

[7] L. M. Woods, T. L. Reinecke, and Y. Lyanda-Geller, Phys. Rev. B **66**, 161318(R) (2002).

[8] G. Burkard and D. Loss, in *Semiconductor Spintronics and Quantum Computation*, edited by D. D. Awschalom, D. Loss, and N.

Samarth (Springer, New York, 2002).
[9] R. de Sousa and S. Das Sarma, Phys. Rev. B **67**, 033301 (2003).
[10] Y. G. Semenov and K. W. Kim, Phys. Rev. B **67**, 073301 (2003).
[11] L. S. Levitov and E. I. Rashba, Phys. Rev. B **67**, 115324 (2003).
[12] A. Khaetskii, D. Loss, and L. Glazman, Phys. Rev. B **67**, 195329 (2003).
[13] B. A. Glavin and K. W. Kim, Phys. Rev. B **68**, 045308 (2003).
[14] S. Dickmann and P. Hawrylak, JETP Lett. **77**, 30 (2003).
[15] J. L. Cheng, M. W. Wu, and C. Lü, Phys. Rev. B **69**, 115318 (2004).
[16] Y. G. Semenov and K. W. Kim, Phys. Rev. Lett. **92**, 026601 (2004).
[17] V. N. Golovach, A. Khaetskii, and D. Loss, Phys. Rev. Lett. **93**, 016601 (2004).
[18] V. A. Abalmassov and F. Marquardt, Phys. Rev. B **70**, 075313 (2004).
[19] E. Tsitsishvili, G. S. Lozano, and A. O. Gogolin, Phys. Rev. B **70**, 115316 (2004).
[20] W. A. Coish and D. Loss, Phys. Rev. B **70**, 195340 (2004).
[21] C.-H. Chang, A. G. Mal'shukov, and K. A. Chao, Phys. Rev. B **70**, 245309 (2004).
[22] D. V. Bulaev and D. Loss, Phys. Rev. B **71**, 205324 (2005).
[23] F. Marquardt and V. A. Abalmassov, Phys. Rev. B **71**, 165325 (2005).
[24] C. F. Destefani and S. E. Ulloa, Phys. Rev. B **72**, 115326 (2005).
[25] J. A. Gupta, D. D. Awschalom, X. Peng, and A. P. Alivisatos, Phys. Rev. B **59**, R10421 (1999).
[26] T. Fujisawa, D. G. Austing, Y. Tokura, Y. Hirayama, and S. Tarucha, Nature (London) **419**, 278 (2002).
[27] T. Fujisawa, D. G. Austing, Y. Tokura, Y. Hirayama, and S. Tarucha, Phys. Rev. Lett. **88**, 236802 (2002).
[28] R. Hanson, B. Witkamp, L. M. K. Vandersypen, L. H. Willems van Beveren, J. M. Elzerman, and L. P. Kouwenhoven, Phys. Rev. Lett. **91**, 196802 (2003).
[29] A. Tackeuchi, R. Ohtsubo, K. Yamaguchi, M. Murayama, T. Kitamura, T. Kuroda, and T. Takagahara, Appl. Phys. Lett. **84**, 3576 (2004).
[30] C. M. Lieber, Nano Lett. **2**, 81 (2002).
[31] B. J. Ohlsson, M. T. Björk, M. H. Magnusson, K. Deppert, L. Samuelson, and L. R. Wallenberg, Appl. Phys. Lett. **79**, 3335 (2001). M. T. Björk, B. J. Ohlsson, T. Sass, A. I. Persson, C. Thelander, M. H. Magnusson, K. Deppert, L. R. Wallenberg, and L. Samuelson, Nano Lett. **2**, 87 (2002).
[32] M. T. Björk, C. Thelander, A. E. Hansen, L. E. Jensen, M. W. Larsson, L. R. Wallenberg, and L. Samuelson, Nano Lett. **4**, 1621 (2004).
[33] Y. Wu, R. Fan, and P. Yang, Nano Lett. **2**, 83 (2002).
[34] A. M. Morales and C. M. Lieber, Science **279**, 208 (1998).
[35] C. L. Romano, S. E. Ulloa, and P. I. Tamborenea, Phys. Rev. B **71**, 035336 (2005).
[36] A. Bertoni, M. Rontani, G. Goldoni, F. Troiani, and E. Molinari, Appl. Phys. Lett. **85**, 4729 (2004).
[37] E. I. Rashba, Sov. Phys. Solid State **2**, 1109 (1960).
[38] Y. A. Bychkov and E. I. Rashba, JETP Lett. **39**, 78 (1984); J. Phys. C **17**, 6039 (1984).
[39] As discussed by R. Winkler [Physica E (Amsterdam) **22**, 450 (2004)] these are the valence band fields produced by the lateral confinement potential, averaged over the conduction band wave functions.
[40] The strong *xy* confinement of the nanowhisker suppresses diamagnetic effects for the weak *B* fields we consider here.
[41] G. D. Mahan, *Many Particle Physics* (Plenum, New York, 1981).
[42] Constants used in the calculation for different materials are as follows. For InSb: $m^*=0.013$, $g_0=-51$, $\gamma_R=500$ Å^2, $\gamma_D=220$ eV Å^3, $\Xi_0=7$ eV, $c_{LA}=3.41$ km/s, $c_{TA}=2.29$ km/s, $D=5.77\times10^3$ kg/m^3, $\kappa=15.7$, and $eh_{14}=0.061$ eV/Å. For GaAs: $m^*=0.067$, $g_0=-0.44$, $\gamma_R=4.4$ Å^2, $\gamma_D=24$ eV Å^3, $\Xi_0=11$ eV, $c_{LA}=4.73$ km/s, $c_{TA}=3.35$ km/s, $D=5.32\times10^3$ kg/m^3, $\kappa=10.3$, and $eh_{14}=0.140$ eV/Å.